Représentation quasicontinue d'un crystal phononique unidimensionnel en un métamatériau acoustique.

Miguel Charlotte, Joseph Morlier

▶ **To cite this version:**

Miguel Charlotte, Joseph Morlier. Représentation quasicontinue d'un crystal phononique unidimensionnel en un métamatériau acoustique.. CFM 2013 - 21ème Congrès Français de Mécanique, Aug 2013, Bordeaux, France. hal-03441341

HAL Id: hal-03441341
https://hal.science/hal-03441341

Submitted on 22 Nov 2021

HAL is a multi-disciplinary open access archive for the deposit and dissemination of scientific research documents, whether they are published or not. The documents may come from teaching and research institutions in France or abroad, or from public or private research centers.

L'archive ouverte pluridisciplinaire **HAL**, est destinée au dépôt et à la diffusion de documents scientifiques de niveau recherche, publiés ou non, émanant des établissements d'enseignement et de recherche français ou étrangers, des laboratoires publics ou privés.

Représentation quasicontinue d'un crystal phononique unidimensionnel en un métamatériau acoustique

M. Charlotte[a], J. Morlier[a]

a. *Université de Toulouse ; INSA, UPS, EMAC, ISAE ; ICA (Institut Clément Ader) ; 10 av. E. Belin, 31055 Toulouse, France*

Résumé :

*L'optimisation des structures à travers le choix ou la conception de (méta-)matériaux multifonctionnels comme la miniaturisation des dispositifs d'ingénierie requièrent une meilleure compréhension analytique des propriétés dynamiques – collectives, anti-continues ou filtrantes – des systèmes complexes (*i.e. *à microstructures) impliqués et nécessitent de choisir ou proposer des modélisations continues locales et/ou homogénéisées plus pertinentes et réalistes que celles utilisées actuellement dans les milieux industrielles et académiques. Pour illustration, nous présentons et analysons les propriétés spectrales et temporelles d'un modèle de chaîne diatomique servant de filtre d'ondes acoustiques pour en déduire, notamment selon la méthode de continualisation proposée récemment par Charlotte et Truskinovsky, ses modélisations quasicontinues multi-échelles, équivalente (nonlocale en espace et en temps, et multi-champs) et homogénéisée (locale en espace et nonlocale en temps et mono-champ). En particulier, nous montrons que ces modèles continus enrichis permettent d'éviter les interprétations matérielles effectives "irréalistes" (par exemple, de masse ou de raideur élastique négative) de la théorie des milieux continus classiques rencontrées dans la littérature. Ces types de modélisation sont des briques essentielles pour obtenir des métamatériaux acoustiques phoniquement optimisés, notamment en utilisant un couplage direct avec des outils d'optimisation topologique (distribution optimale de matière pour atteindre un objectif, ici atteindre un gabarit spécifique de fonction de transfert).*

Abstract :

Optimizing structures through the selection or design of multifunctional (meta-)materials as well as miniaturizing engineering devices require a good analytical understanding of the collective, anti-continuous, or filtering dynamic properties of the involved complex systems with microstructures. They also need to choose or propose continuous modelings that are more pertinent and realistic than those currently used. This work focuses on the basic physics and acoustic bandgap properties of Phononic crystals in order to extract their main mechanical features from homogeneous and enhanced continuum viewpoints. We notably revisit the Born's diatomic chain model in order to clarify certain aspects of its temporal and spectral properties and proposes an equivalent multi-scale quasicontinuum (that is nonlocal in both space and time, and multi-fields) and homogenized one (that is local in space and nonlocal in time, and monofield) which may help to bridge the gap between standard continuum model and granular (or atomic) physics used as acoustic-wave filters.

Mots clefs : cristaux phononiques ; métamatériaux acoustiques ; continualisations.

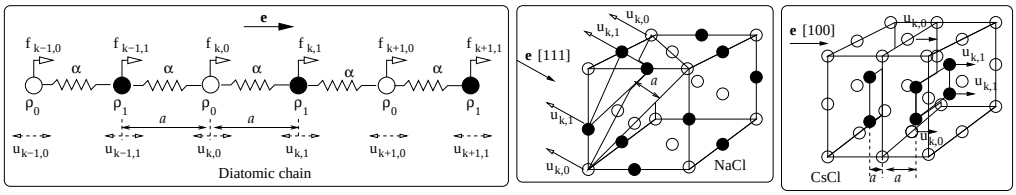

FIGURE 1 – *The 1D-diatomic crystal lattice and its 3D counterparts. In the 3D cases,* $\bar{a} = 2a$ *represents the interreticular plane distance towards which the plane-waves propagate parallely to the wave-vector direction* **e** *(oriented according to the NaCl-*[111] *and CsCl-*[100] *crystallographic plane directions).*

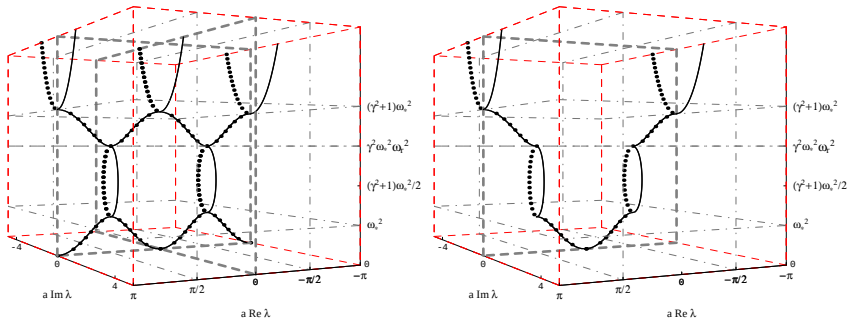

(a) 1D diatomic PnC case (b) Effective active AMM case

FIGURE 2 – *The complex structure of the dispersion relation of the 1D diatomic PnC intercepted by the domain* $\mathbb{B}_0 \times \omega_*^2\mathbb{R}^+$ in (a) *is formed by overlapping the acoustic dispersion curve* $\left(\lambda_o(\omega_r), \omega_r^2\right)$ *of the effective active monoatomic AMM in* (b) *with the one-half intercepted portions of the two optical dispersion curves* $\left(\lambda_o(\omega_r) \pm \pi/a, \omega_r^2\right)$ *that lie inside the strip* $\mathbb{B}_0 \times \omega_*^2\mathbb{R}^+$ *;* $\omega_r \in \omega_*\mathbb{R}$.

1 Introduction

Phononic crystals (**PnCs**) are composite periodic structures with modulated material properties that produce frequency (or phononic) bandgaps (**PnBGs**), *i.e.* frequency regimes where the elastic or acoustic waves can not propagate [10]. In recent years, increasing effort has been devoted to the development of artificial PnCs that similarly suppress, control, guide or localize elastic or sound wave vibrations, while focusing the analysis mainly on the propagation of classical waves in such media. These PnCs can be either *passive filters* that are usually built with periodic composite materials or *active filters* that are built from actuators (*e.g.* PZT). In view of their growing potential applications as beam splitters, sound or vibration protection devices, or waveguides, it may become important to identify from a sound continuum viewpoint the most fundamental concepts and rules that govern the behavior of these materials in order to use its powerful analytical and numerical tools. Only few works have attempted to provide a consistent continuous modeling to these frequency-filtering materials, which can be viewed as *acoustic metamaterials* (**AMMs**), *i.e.* artificially tuned materials that display unusual macroscopic properties or homogenized material parameters as negative mass densities or elastic stiffnesses [7, 8]. As it is outlined here, such an analysis may be relevant for developing enhanced continuum models [3, 5, 6, 8, 9, 11, 12] that are more suitable at nano- and meso-scales [4] and allow to avoid the inconsistent interpretations of the classical homogenized continuum theories.

2 Diatomic (phononic) chain model

The simplest natural PnCs for which an exact (one-dimensional) quasi-continuum modeling can be derived corresponds to Born's unbounded diatomic chain model (cf. Fig. 1) for waves propagating in ionic crystals such as NaCl or CsCl [1]. In this unbounded chain of identical cells of atoms, each cell is made of two types of atoms : within the k^{th} unit-cell (with $k \in \mathbb{Z}$), $\rho_p a$ (with $p = 0, 1$) denotes the mass of atom indexed with (k, p), while $\rho_p > 0$ represents some lineic mass density along the chain direction $\mathbf{e}$. For simplicity, each atom interacts only with its nearest neighbors through linear elastic interaction bond modeled as weightless springs with (strictly positive or negative) their stiffness αa defined with an elastic modulus $\alpha > 0$. The previous material constants are introduced with an arbitrary (small or large) lattice length scale $a > 0$ and arbitrary lineic mass densities but we consider without loss of generality the mass ratio $\gamma \stackrel{\text{def}}{=} \sqrt{\frac{\rho_0}{\rho_1}} > 1$. We can define from these material constants the first acoustic cut-off angular frequency ω_* which set the reference time $\omega_*^{-1} \stackrel{\text{def}}{=} \frac{a}{2}\sqrt{\frac{2\rho_0}{\alpha}} = \frac{a}{2\hat{c}_*}$, for waves propagating in the diatomic chain at the characteristic acoustic velocity $\hat{c}_* \stackrel{\text{def}}{=} \sqrt{\frac{\alpha}{2\rho_0}}$ over a primitive diatomic cell of size $\bar{a} \stackrel{\text{def}}{=} 2a$. Two other interesting reference times characterize waves propagating at optical velocities over the unit-diatomic cell that are related with the minimal optical angular frequency $\omega_m \stackrel{\text{def}}{=} \gamma\omega_* = \frac{2\hat{c}_m}{a}$ and the maximal optical angular frequency $\omega_h \stackrel{\text{def}}{=} \sqrt{\gamma^2+1}\,\omega_* = \frac{2\hat{c}_h}{a}$.
The time-dependent displacements and velocities of the k^{th}-unit cell atoms $((k,p))_{p\in\{0,1\}}$, and the related couple of external forces that are arbitrary imposed on those atoms, are respectively denoted

$$\mathbf{u}_k(t) = \left[\begin{array}{c} u_{k,0}(t) \\ u_{k,1}(t) \end{array}\right],\ D_t\mathbf{u}_k(t) = \left[\begin{array}{c} D_t u_{k,0}(t) \\ D_t u_{k,1}(t) \end{array}\right] \text{ and } a\mathbf{f}_k(t) = \left[\begin{array}{c} a f_{k,0}(t) \\ a f_{k,1}(t) \end{array}\right] \text{ for } (k,t) \in \mathbb{Z}\times\omega_*^{-1}\mathbb{R}.$$

For conciseness here the chain is assumed initially at rest, the evolution of the chain from any arbitrary given initial atomic positions and velocity will be presented elsewhere ; the external forces are causal, with their time-support on $\omega_*^{-1}\mathbb{R}^+$, and sufficient decreasing with respect to the time variable $t \geq 0$ and lattice space variable $ka \in a\mathbb{Z}$. Lately, we assume that no atomic collision and singular time-impulse loading are allowed in our analysis for simplicity and clarity. The dynamic motion of the chain can be described within the framework of the generalized function theory of causal evolutions, as the solution of the following Cauchy's evolution problem for $(k,p,t) \in \mathbb{Z}\times\{0,1\}\times\omega_*^{-1}\mathbb{R}^+$

$$\rho_p\, D_t^2 u_{k,p} = \frac{\alpha}{a^2}\big[u_{k+p,1-p} + u_{k+p-1,1-p} - 2u_{k,p}\big] + f_{k,p}\ ,\ \text{with } \mathbf{u}_k(0) = \omega_*^{-1} D_t\mathbf{u}_k(0) = \mathbf{0}\,. \tag{1}$$

The solution $\{\mathbf{u}_k(t)\}_{k\in\mathbb{Z}}$ and the dynamical material properties of the chain can be characterized by combining the Laplace's transform in time and a Discrete Fourier's transform in space, yielding then

$$u_{k,p}(t) \equiv \sum_{q=0,1} \tilde{u}_{2k+p,q}(t)\ ;\ \left[\begin{array}{c} \tilde{u}_{k,0}(t) \\ \tilde{u}_{k,1}(t) \end{array}\right] \stackrel{\text{def}}{=} \sum_{(q,j)\in\mathbb{Z}^2} \int_0^t \frac{1}{\rho_0}\mathbf{G}((k-j)a, t-\hat{t}) \left[\begin{array}{c} f_{q,0}(\hat{t})\delta_{(j-2q,0)} \\ f_{q,1}(\hat{t})\delta_{(j-2q,1)} \end{array}\right] d\hat{t} \tag{2}$$

with for $(s,t) \in a\mathbb{R}\times\omega_*^{-1}\mathbb{R}$ and $\mathcal{C} \stackrel{\text{def}}{=} \left]-\infty,-\omega_h\right] \cup \left]-\omega_m,-\omega_*\right] \cup \left[\omega_*,\omega_m\right] \cup \left[\omega_h,\infty\right[$

$$\mathbf{G}(s,t) \stackrel{\text{def}}{=} \frac{1}{2\pi}\int_{-i\omega_b-\infty}^{-i\omega_b+\infty} \left[\begin{array}{cc} g_{0,0}(s,\omega)\,\cos^2(s\pi/\bar{a}) & \gamma\, g_{0,1}(s,\omega)\,\sin^2(s\pi/\bar{a}) \\ \gamma\, g_{1,0}(s,\omega)\,\sin^2(s\pi/\bar{a}) & \gamma^2 g_{1,1}(s,\omega)\,\cos^2(s\pi/\bar{a}) \end{array}\right] \mathrm{e}^{i\omega t}\, d\omega\ , \tag{3}$$

$$g_{p,q}(s,\omega) \stackrel{\text{def}}{=} \frac{\mathrm{e}^{i|s|\lambda_0}\left[1-\delta_{p,q}+\delta_{p,1}\delta_{q,1}\frac{\sqrt{\omega_*^2-\omega^2}}{\sqrt{\omega_m^2-\omega^2}}+\delta_{p,0}\delta_{q,0}\frac{\sqrt{\omega_m^2-\omega^2}}{\sqrt{\omega_*^2-\omega^2}}\right]}{i\omega\sqrt{\omega_h^2-\omega^2}}\ ,\ \text{for } \omega\in\omega_*\mathbb{C}\setminus(\mathcal{C}\cup\{0\}) \tag{4}$$

$$\lambda_0(\omega) \stackrel{\text{def}}{=} \frac{i}{a}\log\left(\sqrt{1-\frac{\omega^2}{\omega_*^2}}\sqrt{1-\frac{\omega^2}{\omega_m^2}}+i\frac{\omega_h\omega}{\omega_*\omega_m}\sqrt{1-\frac{\omega^2}{\omega_h^2}}\right)\ ,\ \text{for}\ \left\{\begin{array}{c} \omega\in\omega_*\mathbb{C}\setminus\mathcal{C} \\ \text{with } |\Re e(\lambda_0)|a \leq \pi \end{array}\right. . \tag{5}$$

Here $\omega_b < 0$ is an arbitrary constant real number with sufficiently large amplitude to ensure the Green function $G(s,t)$ in (3) is causal ; $\delta_{p,q}$ with $(p,q) \in \mathbb{Z}^2$ represents Kronecker's delta symbol ; the principal determinations of the complex multiform square-root and logarithm functions are used, with notably $i \stackrel{\text{def}}{=} \sqrt{-1}$; $\Re e(\cdot)$ represents the real part of the complex function or number in argument. The complex function $\lambda_0(\omega)$ describes for $\omega \in \omega_* \mathbb{R}$ the dispersion curves depicted in Fig. 2(b). Its image stands over the complex strip domain $\mathbb{B}_0 \stackrel{\text{def}}{=} \left\{\lambda = \lambda_r + i\lambda_i \in a^{-1}\mathbb{C} \text{ s.t. } (\lambda_r a, \lambda_i a) \in \mathbb{R}^2 \text{ with } \lambda_r \in \mathbb{K}_0\right\}$ that contains both the first Brillouin zone $\overline{\mathbb{K}}_0 \stackrel{\text{def}}{=} [-\pi/\bar{a}, \pi/\bar{a}]$ of the diatomic chain with unit cells of size $\bar{a}$ and the one $\mathbb{K}_0 \stackrel{\text{def}}{=} [-\pi/a, \pi/a]$ of a homogeneous monoatomic chain with unit cells of size a ; here, $\lambda_0(\omega)$ and its translations $\lambda_0(\omega) \pm \pi/a$ generate over $\overline{\mathbb{K}}_0$ respectively the well-known acoustic and optical branches of the dispersion curves of the diatomic PnC that are plotted in Fig. 2(a). According to that solution, the waves with angular frequencies ω in the PnBG domain $\mathcal{C}$ are attenuated/evanescent, while those with $\omega \in \omega_* \mathbb{R} \setminus \mathcal{C}$ are allowed to propagate through the chain.

3 Equivalent multifield quasicontinuum

The methodology developed in [2] allows to identify the following nonlocal multi-field quasi-continuum (**QC**) modeling for the canonic displacements $\tilde{\mathbf{u}}_k(t) = \left[\begin{array}{c} \tilde{u}_{k,0}(t) \\ \tilde{u}_{k,1}(t) \end{array}\right]$ of the previous PnC

$$\begin{array}{l} \displaystyle\int_0^t \int_{a\mathbb{R}} \left[\mathbf{\Phi}_L(s-\hat{s}, t-\hat{t}) + \mathbf{\Phi}_{NL}(s-\hat{s}, t-\hat{t})\right] \mathbf{u}(\hat{s},\hat{t})\, d\hat{s}\, d\hat{t} = \mathbf{f}(s,t) \ , \text{ for } (s,t) \in a\mathbb{R} \times \omega_*^{-1}\mathbb{R} \\ \text{with } \mathbf{u}(s,0) = \omega_*^{-1} D_t \mathbf{u}(s,0) = \mathbf{0} \, , \end{array} \tag{6}$$

what reminisces those in [3, 6, 11, 12]. Eq. (6) relates the displacement field vector $\mathbf{u}(s,t) = \left[\begin{array}{c} u_0(s,t) \\ u_1(s,t) \end{array}\right]$ to the spatially localized loading force density vector $\mathbf{f}(s,t) = \displaystyle\sum_{q\in\mathbb{Z}} \left[\begin{array}{c} f_{q,0}(t)\delta(s/a - 2q) \\ f_{q,1}(t)\delta(s/a - 2q - 1) \end{array}\right]$ defined with the Dirac's generalized function $\delta(s) \stackrel{\text{def}}{=} D_s^2 \frac{|s|}{2}$, while using a couple of generalized field matrices

$$\left\{\begin{array}{c} \mathbf{\Phi}_L(s,t) \\ \mathbf{\Phi}_{NL}(s,t) \end{array}\right\} \stackrel{\text{def}}{=} \frac{1}{2\pi} \int_{-i\omega_b - \infty}^{-i\omega_b + \infty} \left\{\begin{array}{c} \mathbf{\Phi}_L(s,\omega) \\ \mathbf{\Phi}_{NL}(s,\omega) \end{array}\right\} \mathrm{e}^{i\omega t} d\omega \ , \text{ for } (s,t) \in a\mathbb{R} \times \omega_*^{-1}\mathbb{R} \tag{7}$$

as spatially-local and -nonlocal integro-differential operators, with

$$\mathbf{\Phi}_L(s,\omega) \stackrel{\text{def}}{=} \frac{\omega}{2\lambda_0} \sqrt{\frac{\omega_h^2 - \omega^2}{\omega_*^2 \omega_m^2}} \left[\begin{array}{cc} \frac{\gamma\sqrt{\omega_*^2-\omega^2}}{\sqrt{\omega_m^2-\omega^2}} \left(\lambda_0^2 - \frac{\pi^2}{2a^2} + D_s^2\right) & \frac{\pi^2}{2a^2} \\ \frac{\pi^2}{2a^2} & \frac{\sqrt{\omega_m^2-\omega^2}}{\gamma\sqrt{\omega_*^2-\omega^2}} \left(\lambda_0^2 - \frac{\pi^2}{2a^2} + D_s^2\right) \end{array}\right] \delta(s) \tag{8}$$

$$\mathbf{\Phi}_{NL}(s,\omega) \stackrel{\text{def}}{=} \frac{\omega}{2\lambda_0} \sqrt{\frac{\omega_h^2 - \omega^2}{\omega_*^2 \omega_m^2}} \left[\begin{array}{cc} \frac{\gamma\sqrt{\omega_*^2-\omega^2}}{\sqrt{\omega_m^2-\omega^2}} & -1 \\ -1 & \frac{\sqrt{\omega_m^2-\omega^2}}{\gamma\sqrt{\omega_*^2-\omega^2}} \end{array}\right] \frac{\pi^2}{a^2} \frac{D_s^2 \mathrm{e}^{i|s|\sqrt{\lambda_o^2 - \pi^2/a^2}}}{i\sqrt{\lambda_o^2 - \pi^2/a^2}} \ , \tag{9}$$

for $\Im m(\omega) < 0$, $\Im m(\cdot)$ representing the imaginary part of the complex function or number in argument. This elastodynamic model of generalized functions can further be decomposed into specific generalized mass and elastic density matrices, following [2]. More interestingly, Eq. (6) is solved by

$$\mathbf{u}(s,t) = \int_0^t \int_{a\mathbb{R}} \mathbf{G}(s-\hat{s}, t-\hat{t})\, \mathbf{f}(\hat{s},\hat{t}) \frac{d\hat{s}}{\rho_0 a}\, d\hat{t} \ , \text{ for } (s,t) \in a\mathbb{R} \times \omega_*^{-1}\mathbb{R} \, , \tag{10}$$

which provides exact interpolations of the discrete displacement vectors in (2), with $\mathbf{u}(ka,t) = \tilde{\mathbf{u}}_k(t)$ and $u((2k+p)a,t) = u_{k,p}(t)$, while $u(s,t) \stackrel{\text{def}}{=} u_0(s,t) + u_1(s,t)$ and $(k,s,t) \in \mathbb{Z} \times a\mathbb{R} \times \omega_*^{-1}\mathbb{R}$.

4 Effective monofield homogeneization and continualization

Effective homogeneous chain with simple structures. Dealing with infinite domains of interaction as in the previous QC model may not be very convenient for some numerical applications. As an alternative, we have investigated the possibility of deriving an effective model of homogeneous monoatomic chain with a time-dependent elastic modulus $\bar{\alpha}(t)$ and a lattice parameter (*i.e.* reference interstice distance) a separating *representative atoms* (**repatoms**) for cells of mass $\bar{\rho}\,a$, with a lineic mass density $\bar{\rho} \overset{\text{def}}{=} \rho_0 + \rho_1$. Here these repatoms/cells are not necessary physical and must be defined with respect to the diatomic unit cells. Bearing in mind that every choice of repatoms/cells may play a crucial role in the dynamic micro-movement to reproduce, for comparison we leave free the local definitions of these repatoms while imposing the global equivalence $\sum_{k\in\mathbb{Z}} a\bar{f}_k \equiv \sum_{k\in\mathbb{Z}} a(f_{k,0} + f_{k,1})$ for the effective external loads $a\bar{\mathbf{f}} = \{a\bar{f}_k(t)\}_{k\in\mathbb{Z}}$ that act on them, with $a\bar{f}_k$ as the load exerted on the k^{th} repatom : for instance, a simple common choice of repatom is the symmetric cell centered at the atom type with the mass $\rho_p a$ (with $p = 0$ or 1) and including two one-halves of the neighbouring atom type with the mass $\rho_{1-p}a$ (e.g. as in [1]), so that the natural load to apply on the k^{th} repatom is $a\bar{f}_k = a[f_{k,p} + (f_{k+p,1-p} + f_{k+p-1,1-p})/2]$; another common choice is the asymmetric cell centered at the center of mass of a diatomic unit cell (e.g. as in [6]), so that the natural load to apply on the k^{th} repatom is $a\bar{f}_k = a(f_{k,p} + f_{k+p,1-p})$.

Besides, the displacements of those repatoms $\bar{\mathbf{u}}(t) = \{\bar{u}_k(t)\}_{k\in\mathbb{Z}}$ are simultaneously constrained by specific linearly elastic, time varying interactions between nearest neighboring (NN) atoms. More explicitly, these interactions are set so as to allow a perfect match with the acoustic branches of the dispersion curves defined by the complex wavenumber function $\lambda_o(\omega)$ in (5) and depicted on Fig. 2(b). The equation of motion for this effective AMM comes then as follows for $(k,t) \in \mathbb{Z}\times\omega_*^{-1}\mathbb{R}$

$$\begin{array}{l} \bar{\rho}D_t^2\bar{u}_k(t) = \displaystyle\int_0^t \frac{1}{a^2}\big[\bar{u}_{k+1}(t-\hat{t}) + \bar{u}_{k-1}(t-\hat{t}) - 2\bar{u}_k(t-\hat{t})\big]\, D_t\bar{\alpha}(\hat{t})\, d\hat{t} + \bar{f}_k(t)\ , \\ \text{with } \bar{u}_k(0) = \omega_*^{-1}D_t\bar{u}_k(0) = 0\ ,\ \text{for } k\in\mathbb{Z} \end{array} \tag{11}$$

$$\text{the time-dependent elastic modulus being like } \bar{\alpha}(t) \overset{\text{def}}{=} \frac{\bar{\rho}a^2}{4\pi}\int_{-i\omega_b-\infty}^{-i\omega_b+\infty} \frac{i\omega\,\mathrm{e}^{i\omega t}}{\cos(\lambda_0 a) - 1}\, d\omega \geq 0 \tag{12}$$

and asymptotically tends to $\bar{\alpha}_{(+\infty)} = \alpha$. The solution of Eq. (11) is obtained as in [2] and reads like

$$\bar{u}_k(t) \quad = \quad \sum_{p\in\mathbb{Z}} \int_0^t \overline{G}\big((k-p)a, t-\hat{t}\big)\, \frac{\bar{f}_p(\hat{t})}{\bar{\rho}}\, d\hat{t}\ ,\ \text{for } (k,t)\in\mathbb{Z}\times\omega_*^{-1}\mathbb{R} \tag{13}$$

$$\text{with } \overline{G}(s,t) \quad \overset{\text{def}}{=} \quad \frac{1}{2\pi}\int_{-i\omega_b-\infty}^{-i\omega_b+\infty} \frac{1-\cos(\lambda_0 a)}{\omega^2\sin(\lambda_0 a)}\, i\mathrm{e}^{\,i(\omega t + \lambda_0|s|)} d\omega\ ,\ \text{for } (s,t)\in a\mathbb{R}\times\omega_*^{-1}\mathbb{R}\,. \tag{14}$$

Equivalent acoustic QC model. Applying the *continualization* or *continuumization* process in [2] on the model of active AMM in (11) yields the following equivalent Cauchy's problem

$$\begin{array}{l} \displaystyle\int_0^t\int_{a\mathbb{R}} \overline{\Phi}_L(s-\hat{s}, t-\hat{t})\, \bar{u}(\hat{s},\hat{t})\, d\hat{s}\, d\hat{t} = \bar{f}(s,t)\ ,\ \text{for } (s,t)\in a\mathbb{R}\times\omega_*^{-1}\mathbb{R} \\ \text{with } \bar{u}(s,0) = \omega_*^{-1}D_t\bar{u}(s,0) = 0\ ,\ \text{for } s\in a\mathbb{R} \end{array} \tag{15}$$

where the scalar elastodynamic generalized function

$$\overline{\Phi}_L(s,t) \overset{\text{def}}{=} \frac{1}{2\pi}\int_{-i\omega_b-\infty}^{-i\omega_b+\infty} \overline{\Phi}_L(s,\omega)\,\mathrm{e}^{\,i\omega t} d\omega\ ,\ \text{for } (s,t)\in a\mathbb{R}\times\omega_*^{-1}\mathbb{R} \tag{16}$$

$$\text{with } \overline{\Phi}_L(s,\omega) \stackrel{\text{def}}{=} \frac{\bar{\rho}\omega^2 a^2}{\cos(\lambda_0 a)-1}\frac{\sin(\lambda_0 a)}{2\lambda_0 a}\left[D_s^2+\lambda_0^2\right]\delta(s)\ ,\ \text{for } (s,\omega)\in a\mathbb{R}\times(\omega_*\mathbb{C}\setminus\mathcal{C}) \tag{17}$$

can further be decomposed into specific generalized mass and elastic densities, by following [2].
The displacement field that solves the Cauchy problem in (15)

$$\bar{u}(s,t)=\int_0^t\int_{a\mathbb{R}}\overline{G}(s-\hat{s},t-\hat{t})\,\bar{f}(\hat{s},\hat{t})\frac{d\hat{s}}{\bar{\rho}a}\,d\hat{t}\ ,\ \text{for } (s,t)\in a\mathbb{R}\times\omega_*^{-1}\mathbb{R}\,, \tag{18}$$

represents an exact interpolation of the discrete displacement vector in (2), with $\bar{u}(ka,t)=\bar{u}_k(t)$ when the spatially localized loading force densities is singular like $\bar{f}(s,t)=\sum_{k\in\mathbb{Z}}\bar{f}_k(t)\,\delta(s/a-k)$.

5 Conclusions

This paper shortly outlines the main results regarding the continualization of a simple PnC model into an AMM while ensuring the consistence of the model with respect to both the classical stability criteria and physical material interpretations. While the details about the derivation of these models of PnCs and AMMs will be presented in a forthcoming publication, some features of their elastodynamics and rheologic normal stress will be illustrated at the CFM 2013.

Références

[1] Brillouin L. and Parodi M., 1956, *Propagation des ondes dans les milieux periodiques. Masson, Dunod*, Paris.

[2] M. Charlotte and L. Truskinovsky, 2012, *Lattice dynamics from a continuum viewpoint. J. Mech. Phys. Solids*, **60**, pp. 1508-1544.

[3] A.C. Eringen, 2002, *Nonlocal continuum field theories. Springer, New-York* .

[4] J. Fish, 2006, *Bridging the scales in nano engineering and science*, *J. Nanoparticle Research*, **8**, pp. 577-594.

[5] J.A. Krumshansl,1965, *Generalized continuum field representation for lattice vibrations*, In *Lattice Dynamics*, R.F. Wallis, ed. Pergamon, London, pp. 627-634.

[6] I. Kunin, 1982, *Elastic media with microstructure, v.I (One dimensional models)*, *Berlin : Springer.*

[7] H.H. Huang and C.T. Sun,2009, *Wave attenuation mechanism in an acoustic metamaterial with negative effective mass density*, *New Journal of Physics*, **11**, 013003 doi :10.1088/1367-2630/11/1/013003.

[8] G.W. Milton and J.R. Willis, 2007, *On modifications of Newton's second law and linear continuum elastodynamics*, *Proc. R. Soc. of London A*, **463**, pp. 855-880.

[9] A.A. Vasiliev, S.V. Dmitriev, A.R. Bishop and A.E. Miroshnichenko, 2010, *Multi-field approach in mechanics of structural solids*, Int. J. Solids Structures, **47**, no 3-4, pp. 510-525.

[10] J. O. Vasseur, P. A. Deymier, B. Chenni, B. Djafari-Rouhani, L. Dobrzynski and D. Prevost, 2001, *Experimental and Theoretical Evidence for the Existence of Absolute Acoustic Band Gaps in Two-Dimensional Solid Phononic Crystals*, *Phys. Rev. Lett.* **86**, no 14, pp. 3012-3015.

[11] J. R. Willis, 1981, *Variational and related methods for the overall properties of composites. Advanced in Appl. Mech.*, **21**, pp. 1-78.

[12] J. R. Willis, *Dynamics of composites*, 1997, In Suquet P., editor, *Continuum Micromechanics : CISM Courses and Lectures*, No. 377, pp. 265–290. *Springer-Verlag-Wien, New York.*